

Hansen Solubility Parameters (HSPs): A Reliable Tool for Assessing the Selectivity of Pristine and Hybrid Polymer Nanocomposites in the Presence of Volatile Organic Compounds (VOCs) Mixtures

Enric Perarnau Ollé,* Jasmina Casals-Terré, Joan Antoni López Martínez, and Josep Farré-Lladós

Polymeric materials are widely employed for monitoring volatile organic compounds (VOCs). Compared to other sensitive materials, polymers can provide a certain degree of selectivity, based on their chemical affinity with organic solvents. The addition of conductive nanoparticles within the polymer layer is a common practice in recent years to improve the sensitivity of these materials. However, it is still unclear the effect that the nanoparticles have on the selectivity of the polymer membrane and vice versa. The current work proposes a methodology based on the Hansen solubility parameters, for assessing the selectivity of both pristine and hybrid polymer nanocomposites. The impedance response of thin polydimethylsiloxane (PDMS) films is compared to the response of hybrid polymer films, based on the addition of multi-walled carbon nanotubes (MWCNTs). With the addition of just 1 wt.% of MWCNTs, fabricated sensors showcased a significant improvement in sensitivity, faster response times, as well as enhanced classification of non-polar analytes (>22% increase) compared to single PDMS layers. The methodology proposed in this work can be employed in the future to assess and predict the selectivity of polymers in single or array-based gas sensors, microfluidic channels, and other analytical devices for the purpose of VOCs discrimination.

1. Introduction

The monitoring of volatile organic compounds (VOCs) has long been important for applications such as air quality, odor detection, the control of industrial processes, and human health and safety.^[1–4] In recent years, the advancements in micro-fabrication techniques and nanomaterials have fostered the deployment of miniature, portable, and highly sensitive gas sensors, which are able to detect VOCs at very low concentrations.^[5–7]


Nonetheless, one of the most challenging issues for realizing effective gas sensors is to achieve high selectivity in the presence of specific VOCs or groups of analytes in a mixture. There are several approaches to enhance the selective properties of gas sensors. One common method employed in the literature is to tune the sensor to specifically interact with one compound and have near-zero cross-sensitivity to other compounds in the environment. This is generally achieved by modulation of the sensor's temperature (e.g., MOS-based sensors)^[8–10],

or the specific characterization of the sensitive material through nanoparticle doping,^[11] thermal treatment,^[12] or chemical functionalization.^[13,14] Despite the effectiveness of these techniques, they are usually expensive, time- and energy-intensive, and often involve complex and tedious processes, which hinders their implementation on a large scale.

In this context, polymers are a class of materials that exploit their affinity towards some types of VOCs, to provide a certain degree of selectivity to gas sensors in a much simpler and cost-effective manner. Compared to other sensitive materials, polymers also present some advantages, such as low power consumption, long-term stability, biocompatibility, and excellent reversibility.^[15,16] The ability of polymers to absorb VOCs and other gases is well known and has been widely exploited in the past for single gas sensors^[17–20] or in sensor array systems.^[21–23] However, the response of individual polymeric materials is sometimes very poor compared to other sensitive materials. To address this issue, a common practice is the

E. P. Ollé, J. Casals-Terré, J. A. L. Martínez, J. Farré-Lladós
 Department in Mechanical Engineering
 Polytechnical University of Catalonia
 Laboratory of Microsystems & Nanotechnology
 Colom Street 11, Terrassa, Barcelona 08222, Spain
 E-mail: enric.perarnau@upc.edu

E. P. Ollé
 SEAT S.A., R&D department
 A-2, Km 585, Martorell, Barcelona 08760, Spain

 The ORCID identification number(s) for the author(s) of this article can be found under <https://doi.org/10.1002/mame.202200511>

© 2022 The Authors. Macromolecular Materials and Engineering published by Wiley-VCH GmbH. This is an open access article under the terms of the Creative Commons Attribution License, which permits use, distribution and reproduction in any medium, provided the original work is properly cited.

DOI: 10.1002/mame.202200511

addition of nanoparticles within the polymer structure to conform hybrid nanocomposites.^[24–26] Hybrid polymer films still benefit from the advantages of polymers and, in addition, they incorporate a significant improvement in sensitivity, provided by the high surface-to-volume ratio of the nanoparticles. Furthermore, the addition of nanoparticles often contributes to faster response times of the sensor, due to increased porosity of the sensitive polymeric layer.^[27] Although recent studies also reported improvements in the selectivity of hybrid polymer films compared to individual polymers,^[28–30] there is still not a clear methodology to analyze and predict the contribution of the nanoparticles in the discretization power of polymers and vice versa.

The selectivity of polymeric materials is achieved by the different absorption properties of analytes. Recent studies show that the level of analytes' absorption for a certain polymer is principally determined by the solubility of both elements.^[31,32] Since often solubility follows the rule of thumb “like dissolves like”, polymers are expected to show more affinity towards analytes with similar solubility and, therefore, a similar chemical nature. In some studies, polymer-analyte affinity is expressed in terms of the polarity of both elements.^[33] Other studies opt for the Hildebrand and Scott model to compare the solubility of the coating polymer and the vapor analytes.^[34,35] However, all these methods fell short in truly explaining the selectivity of polymeric materials towards VOCs and other gases. To tackle these limitations, Hansen suggested three main parameters that consider all major interactions between gas molecules and a certain polymer^[36]: i) dispersion interactions caused by the Van der Waals forces; ii) dipolar interactions caused by the polarity of the molecule; and iii) hydrogen bonding interactions. These three parameters are additive and give a more complete indication of the solubility of a certain material or molecule, compared to other models.

The current work intends to implement a methodology based on the Hansen solubility parameters (HSPs) to analyze and predict the selectivity of both, pristine and hybrid polymeric materials in presence of common VOCs. The Hansen solubility parameters have already been used in the past to assess the solubility of vapor solvents in polymers^[37–39]; or as a way to evaluate the dispersion and compatibility of nanofillers in organic solvents^[40–42] or in combination with polymers.^[43,44] This work aims to demonstrate that HSPs are also a powerful and reliable tool for the proper selection of polymer composites in the selective detection of gases. Polydimethylsiloxane (PDMS) is employed as the base polymer for the experiments and multi-walled carbon nanotubes (MWCNTs) are selected as the conductive nanofillers, due to their robust mechanical and electronic properties, chemical stability, and large surface area. Both, pristine and hybrid PDMS films are spin-coated on top of micro-gap interdigitated electrodes (M-IDEs), for the creation of a miniaturized chemoresistive gas sensor that operates at room temperature. Fabricated sensors are tested in a controlled environment and in presence of four representative VOCs, with a different chemical affinity toward PDMS: isopropanol (IPA), ethyl acetate (EthAc), methanol (MeOH), and toluene.

These works start by analyzing the performance of pristine PDMS films on top of M-IDEs. In order to understand the effect of the polymer's thickness in the response of the transducer, single PDMS films are initially spin coated at five different thicknesses, ranging from 2.5 μm to 25 μm . Second, MWCNTs are

added and blended into PDMS films at concentrations ranging from 0.1 to 2.0 wt.%, to also understand the effect of nanoparticles' concentration. MWCNTs are scattered within the polymer using a novel technique that employs isopropanol (IPA) as a dispersion solvent, in combination with intense periods of ultrasonication and magnetic stirring.^[45] The responses of the fabricated sensors are analyzed by means of the Impedance Spectroscopy (IS) technique. The IS is an ultra-sensitive method that has recently been considered for the detection of gases, proving a superior performance compared to other conventional methods.^[46–48] This technique is very surface sensitive; hence, it can help to identify processes at the interface between M-IDEs and polymer composites that other techniques are not able to capture.^[49] Besides, the IS allows to analyze the response of both, pristine and hybrid PDMS films with a unique analytical method, which reduces efforts for data interpretation.

In summary, this work aims to present HSPs as a reliable tool to assess and predict the selectivity of polymer composites in presence of organic vapor solvents. The methodology proposed in this work has the potential to be considered in the design phase of single gas sensors, sensor array systems (e-nose), or microfluidic devices that exploit polymeric materials for the purpose of VOCs discrimination.

2. Experimental Section

2.1. Materials

PDMS films are created by mixing the base of Sylgard 184 Silicone Elastomer Kit with the corresponding curing agent, purchased from Dow Inc. Multi-walled carbon nanotubes MWCNTs (>98% carbon basis, length 2.5–20 μm , outer diameter 6–13 nm) were purchased from Sigma Aldrich. Tested analytes were isopropanol, methanol, ethyl acetate, and toluene, all purchased from Sigma Aldrich with a purity $\geq 99.0\%$. M-IDEs were purchased from MicruX Technologies Ltd. M-IDEs are made of gold (Au) and consist of two individually microelectrode array strips with an interdigitated distribution. M-IDEs are deposited on a glass substrate and have the following general dimensions: $10 \times 6 \times 0.75$ mm. They have a thickness of ≈ 150 nm, width (W) ≈ 10 μm , inner gap (G) ≈ 10 μm , and form a total sensing area (A) of 9.62 mm².

2.2. Nanocomposite Films Preparation

For the preparation of pristine PDMS films, the base of Sylgard 184 silicone elastomer was blended with the curing agent in a standard 10:1 weight ratio. The PDMS mixture was then degassed in a vacuum chamber for 15 min until all air bubbles were removed from the composite. On the other hand, for the fabrication of hybrid MWCNTs-PDMS films, a simple, fast, and cost-effective method was adopted. Carbon nanotubes tend to agglomerate and form heavy agglomerations inside the polymer layer. One method widely employed to force the separation of carbon bundles is the stirring of nanoparticles with an appropriate solvent in combination with an ultrasonic treatment.^[50,51] In this work, pristine MWCNTs were dispersed in excess IPA (1000:1),

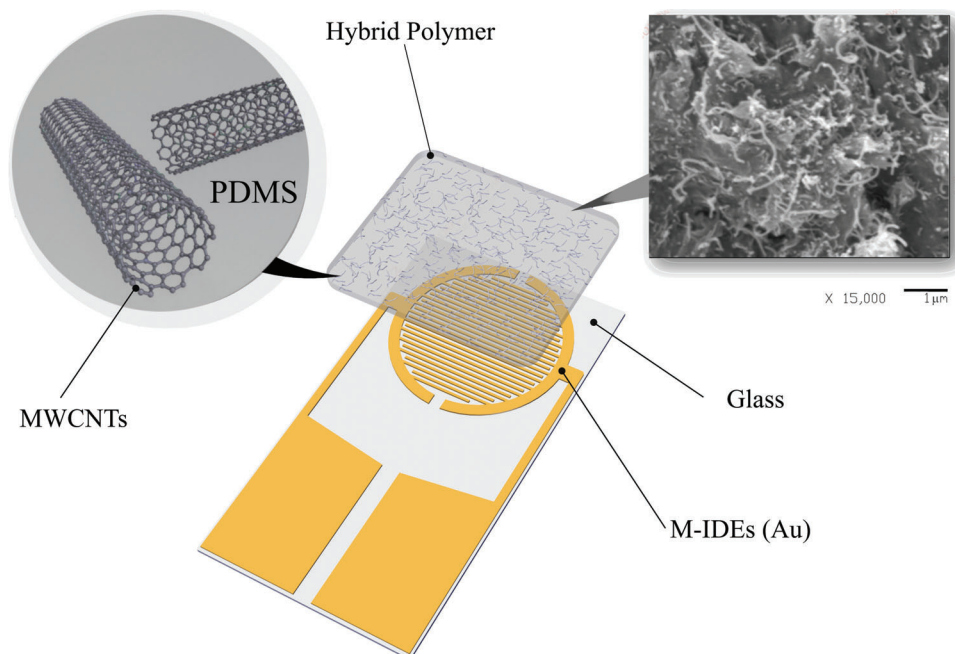


Figure 1. Schematic representation of the MWCNTs-PDMS sensitive layer on top of M-IDEs and SEM image obtained from the fracture surface of one hybrid nanocomposite containing 1.0 wt.% of carbon nanoparticles.

and then submitted to ultrasonication for 30 min and magnetic stirring for 1 h.^[45] Afterward, the base of Sylgard 184 was added and the whole solution was submitted to ultrasonication for 1 h and magnetic stirring for 1–2 h more. Agitation times and solvent concentration were adjusted to ensure a good dispersion of MWCNTs inside the polymer layer, especially at high concentrations of nanoparticles. With this method, a uniform distribution of carbon nanoparticles was achieved inside the PDMS layer (see **Figure 1**). Finally, IPA was vaporized at a low temperature (60 °C) for a period of 1.5 h, to avoid holes in the polymer structure caused by an abrupt evaporation process. Once the solvent was completely evaporated, the curing agent was added and blended to the mixture (10:1). Hybrid polymer films were created at four different concentrations of MWCNTs following the same method: 0.1, 0.5, 1.0, and 2.0 wt.%.

2.3. Fabrication of Sensors

Prior to the deposition of the sensitive films on top of M-IDEs, electrodes were submitted to a surface pre-cleaning. They were immersed in a piranha solution $\text{H}_2\text{SO}_4:\text{H}_2\text{O}_2$ (3:1) for 20 min and rinsed with DI water. M-IDEs were then dried using a constant Nitrogen flow (N_2) and heated at 110 °C in a hot plate for 15 min, to erase any trace of water particles on the surface. For the fabrication of sensors, M-IDEs were placed on top of a crystal plate, using a double-sided tape. To avoid interferences and ensure that sensitive polymer films were only coated on top of the interdigitated fingers, a sacrificial tape layer was used to cover the remaining parts of M-IDEs. Realization of the different polymer films was achieved by the spin-coating technique. Hybrid and pristine PDMS materials were poured on top of electrodes, so that the entire interdigitated surface was covered. The parame-

ters on the spinner (speed, acceleration/deceleration ramps, and time) were set to achieve the desired polymer thickness. Pristine PDMS films were coated at five different thicknesses: 2.5, 5.0, 15.0, 20.0, and 25.0 μm ; whereas a thickness of $\approx 200 \mu\text{m}$ was obtained for hybrid MWCNTs-PDMS films, due to the higher viscosity of the materials. After the deposition of the sensitive material, fabricated sensors were left on a hot plate for 2.5 h at the optimum temperature of 75 °C, to complete the curing process of PDMS.^[52] Finally, the sacrificial tape initially placed on the electrodes was removed and sensors were preserved at controlled environmental conditions for 48 h. All fabrication parameters and two 3D profile pictures of single PDMS films (5 and 20 μm thick) can be found in the supporting material.

2.4. Characterization

2.4.1. Laboratory Setup

A dedicated 28 L gas chamber was prepared to evaluate the performance of fabricated sensors upon exposure to different VOCs. The chamber lid had two small openings, one for the injection of analytes and another for the exit of connection cables. M-IDEs were placed inside the gas chamber on top of a small drop cell holder from MicruX, which was connected via a small USB cable to an EmStat Pico potentiostat from PalmSens BV and then to a PC for data interpretation. A small 5 V fan was incorporated inside the chamber to provide a uniform distribution of analytes in the confined volume. The response of fabricated sensors was evaluated in a clean ambient air atmosphere, under controlled climatic conditions. Initially, sensors were purged and the gas chamber was cleaned up using a constant flow of N_2 for several minutes. The chamber was then closed and isolated with a

sealing gum. Impedance measurements started and the system was left idle for several minutes (5–10 min) to reach baseline conditions. Selected volumes of liquid organic solvents in mL were introduced to the chamber using a pipette. The ventilator was then turned on until analytes' droplets were completely evaporated at room temperature. In all measurements ambient temperature was kept ≈ 23 °C and relative humidity at $\approx 35\%$, with the help of two indicators from ThermoPro. A clear picture of the whole laboratory testing setup can be found in Figure S2 (Supporting Information) of the supporting material. To estimate the gas concentration, in parts per million (ppm), for each of the tested analytes, the following expression was considered^[53]:

$$C = \frac{d \cdot V_a \cdot p \cdot R \cdot T}{M_a \cdot P \cdot V_c} \times 10^{-6} \quad (1)$$

where d , M_a , p , and V_a are density (g mL⁻¹), molecular weight (g mol⁻¹), purity (%), and volume injected (mL) of liquid analytes. T and P are operating temperature and pressure (≈ 1 atm), R is the constant of gases (0.082 L atm K⁻¹ mol⁻¹), and V_c is the volume of clean air in the gas chamber. All chemical properties and calculated concentrations of VOCs can be found in Table S2 (Supporting Information) of the supporting material.

2.4.2. Data Measurements and Interpretation

The response of fabricated sensors was analyzed by the IS technique using the PS Trace 5.8 software tool from PalmSens BV. All measurements were done in a potentiostatic mode. Thus, a small amplitude AC voltage ($E_{AC} \approx 50$ mV) was superimposed on a baseline DC potential, which resulted on a DC current with a superimposed AC current (I_{AC}) as well. All measurements yielded the impedance defined by the general expression: $Z = E_{AC}/I_{AC}$. The real (Z') and imaginary (Z'') parts of impedance were monitored using the Nyquist or Bode plots. Response signals were also analyzed by means of the complex capacitance spectra ($C = C' + C''$), using the expressions defined in.^[54] Initially, the response of fabricated sensors was evaluated over a wide range of frequencies (10–100 kHz). A frequency of 10 kHz was then selected as the most optimum to assess the response of fabricated sensors over time. In this work, experimental data was evaluated by fitting it to an equivalent Electrical Circuit Model (ECM). PS Trace employs the Levenberg-Marquardt algorithm and the chi-squared test (χ^2) to find the best ECM fit to a real system. In this study, the impedance response of pristine PDMS sensors displayed a strong capacitive behavior. The best ECM fit was obtained with a resistor in series with a constant phase element (CPE), which is similar to a regular capacitor, but it incorporates deviations caused by non-ideal coating conditions. Hence, a CPE displayed a much better fit to the real response of the sensor ($\chi^2 \approx 4.84 \times 10^{-6}$) compared to an ideal capacitor ($\chi^2 \approx 1.04 \times 10^{-3}$). On the other hand, the impedance response of hybrid polymer films displayed a dual behavior. At high frequencies, the response of the sensor presented a capacitive dominant behavior; whereas, at low frequencies, the response was very close to a pure resistive element, provided by the high resistivity of MWCNTs. Hence, the best ECM fit in this case was obtained with a CPE and a resistor connected in parallel ($\chi^2 \approx 9.95 \times 10^{-6}$).

More information on the respective ECMs of pristine and hybrid polymer composites can be found in the supporting material. The sensitivity of fabricated sensors (S) was obtained by the linear extrapolation of the response signal over time, which is the ratio between the variation of the steady-state impedance of the sensor (ΔZ) versus the variation in the analyte's concentration (Δc):

$$S = \frac{\Delta Z}{\Delta c} \quad (2)$$

In this work, the limit of detection (LoD) of each sensor was calculated using the ratio $3\sigma_b/S$, where σ_b is the standard deviation of the transducer blank impedance (34–114 Ω) and S is the calculated sensitivity in Ω ppm⁻¹. Finally, in order to compare the discretization power of fabricated sensors, the relative selectivity (s) was defined as the ratio of sensitivities between any compound and a reference analyte (in this case IPA), using this expression:

$$s = \frac{S_n}{S_{IPA}} \quad (3)$$

2.4.3. Selectivity Analysis

In the present work, selectivity was analyzed based on the chemical affinity that each analyte has with the coating polymer, in both, pristine and hybrid composites. In this work, the HSPs were employed to determine the affinity between PDMS and analytes, as well as MWCNTs and analytes. Theoretically, liquids with similar solubility parameters were miscible and, in recent years, it was shown that organic solvents also tend to dissolve better in materials, whose solubility parameters are not too different from each other.^[39] Therefore, in general terms, a solvent-solute pair with similar HSPs should be more miscible and share a higher affinity than a pair with disparate HSPs. As an extension of the Hildebrand and Scott method, Hansen divided the total cohesive energy of a molecule into three major interaction forces: dispersion interactions (δd), dipolar interactions (δp), and hydrogen bonding interactions (δh). These three components are known as the HSPs and are additive to give the general solubility of an element in MPa^{1/2}:

$$\delta t^2 = \delta d^2 + \delta p^2 + \delta h^2 \quad (4)$$

As it was explained before, solubility between two materials normally follows the rule of thumb “like dissolves like.” To measure the similarity between the HSPs of PDMS, MWCNTs, and each organic solvent employed in this work, authors used the equation developed by Skaarup, which determines the affinity between two materials based on the “distance” (Ra) of their respective partial solubility parameters, in MPa^{1/2}.^[36]

$$Ra = \sqrt{4(\delta d_i - \delta d_j)^2 + (\delta p_i - \delta p_j)^2 + (\delta h_i - \delta h_j)^2} \quad (5)$$

where subscripts (i) and (j) refer to the studied material and each organic solvent respectively. According to this method, the smaller the Ra value, the higher the affinity between a certain solvent and a polymer composite, which should result in a higher selectivity of the material. Due to the hydrophobic nature of PDMS, this polymer tends to display higher affinity toward nonpolar or

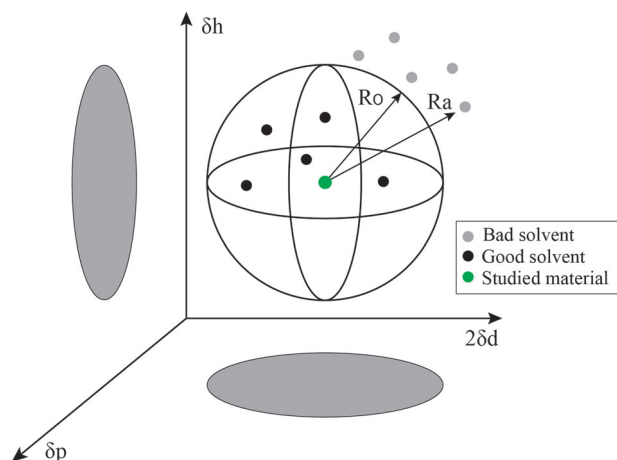


Figure 2. Schematic representation of the Hansen solubility parameters of a studied material in a 3D space.

weakly polar compounds, than analytes with high polarity and/or significant hydrogen bonding properties.^[55] Similar to PDMS, MWCNTs also have a strong nonpolar nature; hence, they should interact better with nonpolar or weakly polar compounds as well. Previous works have reported that MWCNTs tend to dissolve better in presence of organic solvents containing nitrogen, such as amines (CO–N) or amides (NC=O); or in compounds with a cyclic molecular structure, such as some lactones or aromatic hydrocarbons.^[56]

However, recent studies show that in addition to the solubility parameters, there are other factors determining the interaction of carbon nanotubes with organic solvents or other materials, such as surface energy or intermolecular interactions.^[57] The solubility parameters of common organic solvents are widely available for the scientific community. Nonetheless, the HSPs for a certain material or solute are not always known and need to be calculated experimentally. The classical approach consists in testing the studied material in a series of organic solvents with known HSPs. The solvents are then classified as good or bad, depending on whether there is a good interaction with the material or not. The interaction between solvent vapors and polymers is normally evaluated in terms of analyte absorbance or polymer swelling^[39]; whereas the interaction between solvents and MWCNTs is generally expressed in terms of nanotube dispersion.^[41]

To determine the solubility parameters of an unknown material based on this method, HSPs are normally represented in a 3D space, with δd , δp , and δh as reference axes. This representation defines the center of a sphere with radius R_o , which is called the interaction radius and determines the maximum distance between any good solvent and the studied material.^[58] In this representation, R_a can be plotted as the distance from any given solvent (good or bad) to the center of the sphere (see **Figure 2**). The solubility parameters of the material are then calculated by an optimization problem that aims to determine the sphere in the 3D space with the minimum interaction radius (R_c), so that all the good tested solvents stay inside the sphere and all the bad solvents stay outside.^[59,60]

In this work, the HSPs considered for PDMS and MWCNTs were taken from relevant references that employed this method-

ology for calculation (see **Table 1**). Based on these parameters, the R_a value was calculated to determine the affinity between PDMS and analytes (R_{a_1}), as well as MWCNTs and analytes (R_{a_2}), and assess the selectivity of pristine and hybrid polymer films in presence of common vapor solvents. In this work, hybrid polymer composites are fabricated with a very low concentration of MWCNTs, which range from 0.1% to 2.0% in weight ratio. Therefore, the main contribution to the final solubility of hybrid composites can be still attributed to the polymer. Individual contributions of PDMS and MWCNTs to the final solubility of the composite were estimated to be proportional to the weight ratio of each material respectively. Because the performance of pristine PDMS films will be compared to polymer composites containing 1.0 wt.% of carbon nanotubes, a combined R_a value was calculated based on the following relation:

$$R_a_c = (R_{a_1} \cdot 0.98) + (R_{a_2} \cdot 0.01) \quad (6)$$

After analyzing the values in **Table 1**, it can be depicted that the R_a values of single PDMS layers (R_{a_1}) are almost the same compared to the combined R_a values of PDMS with just 1.0 wt.% of MWCNTs (R_a_c), which indicates the minimum impact of the carbon nanoparticles in the total solubility of the polymer composite upon exposure to vapor solvents.

3. Results and Discussion

3.1. Polymer-Coated Micro Interdigitated Electrodes (M-IDEs)

When single layers of PDMS are coated on top of M-IDEs a small capacitor is formed. The response of pristine polymer chemocapacitors is mainly determined by changes in the permittivity (ϵ) of the polymer layer upon exposure to vapor analytes, which trigger a measurable change in the impedance of the device.^[63–65] The geometrical characteristics of both, M-IDEs and the polymer layer are key to understanding the response of these sensors.^[66] In this work, the fundamental geometrical properties of M-IDEs were maintained in all the experiments ($W = G = 10 \mu\text{m}$). In order to study the effect of the polymer thickness (h), M-IDEs were coated at five different thicknesses: 2.5, 5.0, 15.0, 20.0, and 25.0 μm . PDMS films on top of M-IDEs contributed to positive variations in the sensor's capacitance, since a thin layer of air was replaced by a thin layer of higher dielectric polymer. Due to the inverse correlation between capacitance and impedance, thicker polymer films resulted in a gradual reduction of the sensor's baseline impedance, until reaching the saturation value of 20 μm , where changes were no longer detected (see **Figure 3**). At a fixed frequency of 10 kHz, the baseline impedance of naked M-IDEs (Z_0) was measured to be 250.060 k Ω , and it decreased down to 245.301 and 233.710 k Ω , with films of 5 and 25 μm respectively.

Theoretically, the response of polymer chemocapacitors reaches a saturation point at a polymer thickness greater than half of the spatial electrodes' wavelength ($\lambda/2 = W + G$),^[67] which, in this work, corresponding to a PDMS thickness of $\approx 20 \mu\text{m}$. According to the literature, three main physical processes contribute to changes in the permittivity of the polymer layer: i) absorption of analytes; ii) adsorption of gas molecules over the polymer surface; and iii) polymer's swelling effect.^[68–70] Changes in permittivity caused by the absorption of analytes can be positive if

Table 1. Hansen solubility parameters, R_a values, and other relevant chemical properties of PDMS, MWCNTs, and all tested VOCs.

Component	Permittivity [ϵ]	Vapor P. [kPa] ^{b)}	δ_d [MPa ^{1/2}] ^{a)}	δ_p [MPa ^{1/2}] ^{a)}	δ_h [MPa ^{1/2}] ^{a)}	δ_t [MPa ^{1/2}] ^{a)}	R_{a_1} [MPa ^{1/2}]	R_{a_2} [MPa ^{1/2}]	R_{a_c} [MPa ^{1/2}]
Isopropanol	18.2	4.4	15.8	6.1	16.4	23.6	13.15	10.23	13.12
Ethyl acetate	6.02	10.0	15.8	5.3	7.2	18.2	5.77	5.83	5.77
Methanol	32.7	12.9	14.7	12.3	22.3	29.4	21.55	17.19	21.51
Toluene	2.38	3.8	18.0	1.4	2.0	18.2	5.16	8.23	5.19
DI Water	80.0	2.3	15.5	16.0	42.3	47.8	40.83	36.11	40.78
PDMS ^{c)}	2.75	–	15.9	0.1	4.7	16.6	–	9.32	–
MWCNTs ^{d)}	–	–	18.6	7.1	7.8	21.4	9.32	–	–

^{a)} HSPs for solvents taken from^[36,39]; ^{b)} Vapor pressure considered at an average temperature of 23 °C; ^{c)} PDMS values and permittivity taken from the Polymer Data Handbook^[61]; ^{d)} HSPs for MWCNTs taken as the average value of relevant experimental studies.^[57,58,60,62]

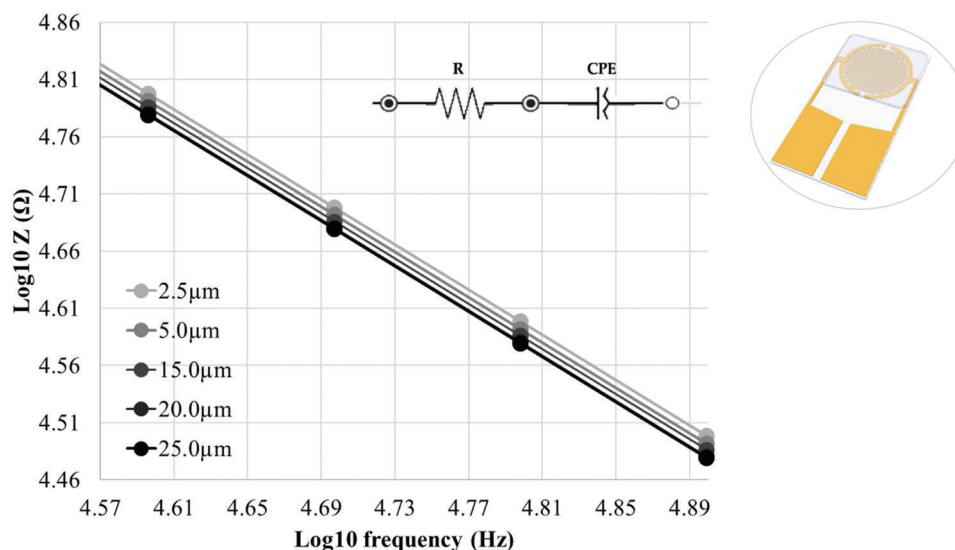


Figure 3. Bode diagram of pristine PDMS films at five different thicknesses: 2.5, 5.0, 15.0, 20.0, and 25.0 μm . The baseline impedance of M-IDEs experiences a gradual reduction with an increase in the polymer thickness, until reaching the saturation value.

the permittivity of analytes is higher than that of the polymer; or negative, if the permittivity is lower. On the other hand, changes in permittivity caused by the adsorption and swelling processes tend to be always positive, since a thin layer of air is replaced by a thin layer of higher dielectric polymer or higher dielectric analyte respectively.^[67] In this study, all tested VOCs have a higher or very similar dielectric constant than PDMS (Table 1). Therefore, pristine PDMS films only displayed neutral or negative variations of impedance ($-\Delta Z$) over time.

Calculated sensitivities (S) and standard deviations (σ) are plotted in **Figure 4**. To ensure a good data sample, two sensors were fabricated at each polymer thickness, and three different measurements were conducted for each of the four tested compounds.

For those analytes with a relatively good affinity with PDMS and a higher permittivity than the polymer layer, sensitivity was measured to increase along with the PDMS thickness. This behavior is normally generalized in the response of pristine polymer chemocapacitors for VOC detection^[69,70] and, in this study, was well-represented by ethyl acetate and IPA compounds. In this case, the response of the sensor is mainly determined by the

absorption of gas molecules in the polymer membrane. An increase in the polymer's thickness contributes to a higher number of electric field lines passing through the sensing film, which usually leads to a greater response. Hence, in the current work, a PDMS thickness of 25 μm is considered optimum for the detection of most VOCs, in terms of sensitivity, signal stability, and to minimize the effect of environmental conditions in all measurements. One indirect effect of increasing PDMS thickness was a reduction in the response times, which is mainly caused by the slower diffusion of gas molecules through thicker polymer films (see **Figure 5**).

Nonetheless, some exceptions were recorded, where thick PDMS films did not lead to the most optimal sensor performance. Toluene, for instance, is a compound with a very high affinity to PDMS, but also with a very similar permittivity. Therefore, the absorption of this analyte in the polymer was barely detected by the transducer. In this case, the greatest sensor response was achieved at thin polymeric films ($h \approx 5 \mu\text{m}$), where changes in permittivity are enhanced by the swelling of the PDMS layer. Another exception occurred in the detection of methanol. Due to the low affinity between PDMS and methanol, the uptake of this

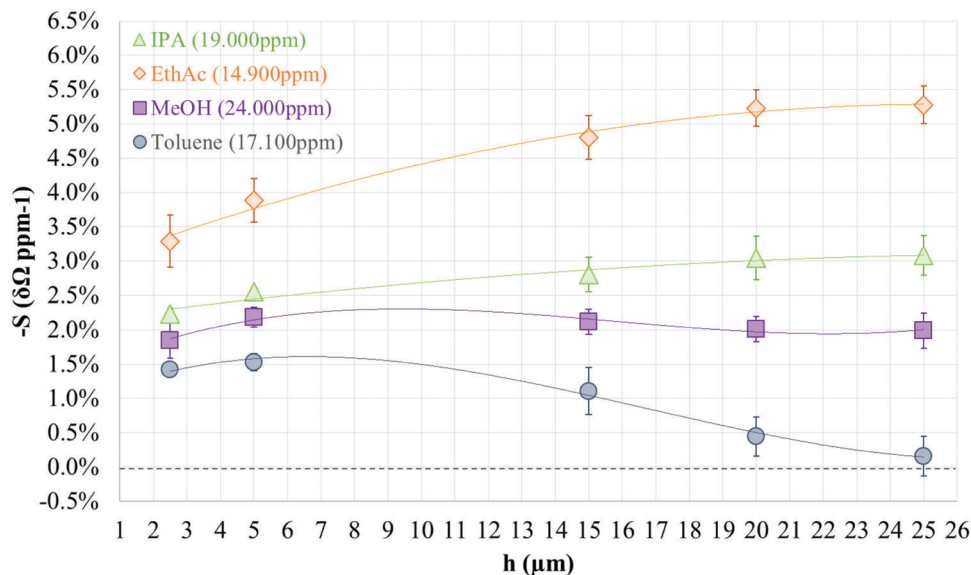


Figure 4. Calculated sensitivities (S) of pristine PDMS sensors at five different polymer thicknesses and in the presence of four VOCs: IPA, ethyl acetate, methanol, and toluene. A polynomial line is used to depict the tendency of measured data points.

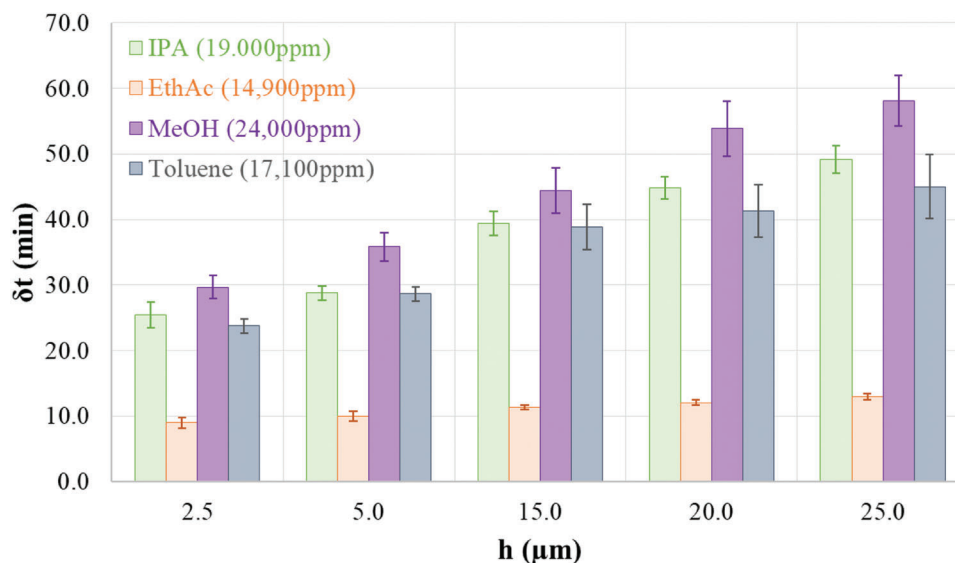


Figure 5. Response times (δt) of pristine PDMS sensors at five different polymer thicknesses and in presence of the four selected VOCs: IPA, ethyl acetate, methanol, and toluene.

analyte is limited at thick polymer films. Hence, the optimum response of the sensor towards methanol was also found to be at a PDMS thickness below the saturation value, where changes in permittivity are enhanced by the adsorption of high dielectric molecules of methanol over the polymer's surface.

3.2. Hybrid MWCNTs-Polymer Coated M-IDEs

When MWCNTs are added within the polymer layer, changes in the impedance of the sensor are mainly triggered by the absorption of analytes and swelling of the polymer film. As the poly-

mer swells, the inter-particle distance between MWCNTs is altered, and some of the conductive paths initially provided by the nanoparticles are partially destroyed.^[71–73] Hence, changes in the impedance of hybrid films are no longer dependent on the permittivity of the polymer, but on the modification of the conductive network provided by the carbon nanoparticles inside the polymer membrane. In order to study the effect of MWCNTs in the response of the device, five different sensors were fabricated at concentrations of nanoparticles varying from 0.1 wt.% to 2.0 wt.% inside the PDMS base material. Hybrid PDMS-MWCNTs films were coated on top of M-IDEs with a thickness of ≈ 200 μm . Think composites were generally preferred in this case, to enhance the

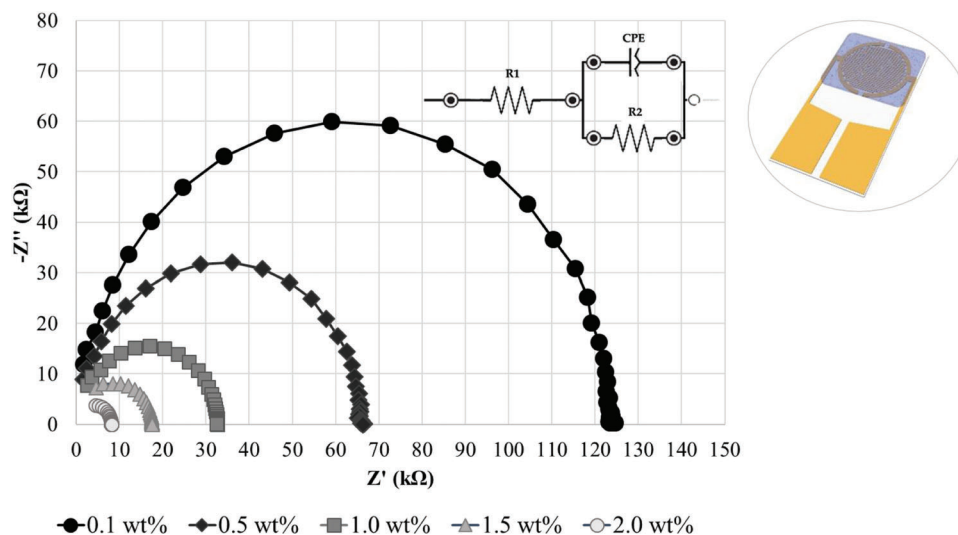


Figure 6. Nyquist diagram of hybrid MWCNTs-PDMS films at five different concentrations of nanoparticles: 0.1, 0.5, 1.0, 1.5, and 2.0 wt.%.

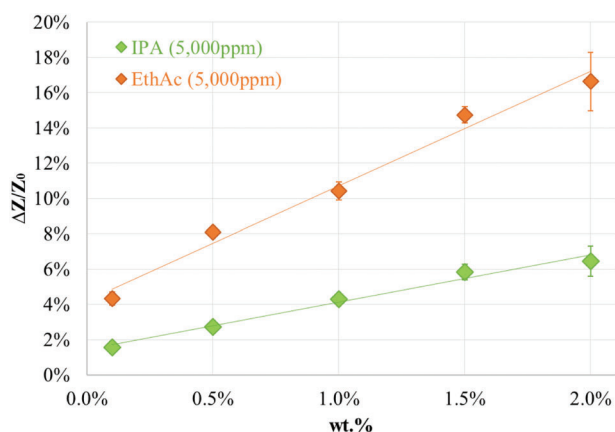


Figure 7. The typical response of fabricated sensors toward 5000 ppm of IPA and ethyl acetate respectively, with concentrations of MWCNTs ranging from 0.1 wt.% to 2.0 wt.%.

absorption of analytes and promote a greater swelling effect. A growing number of conductive fillers increases the formation of conductive paths within the polymer matrix, which contributes to an important reduction of the sensor's baseline impedance (see **Figure 6**). This phenomenon has been reported in previous studies and can be well explained by the percolation theory.^[74,75]

The average baseline impedance (Z_0) of hybrid films containing 0.1 wt.% of MWCNTs was measured to be 108.652 kΩ, and it decrease down to 31.858 and 8.096 kΩ for nanocomposites containing 1.0 and 2.0 wt.% of carbon nanoparticles respectively. Even though composites with a growing number of nanoparticles displayed a slight increase in response (see **Figure 7**), polymers with concentrations >1.0 wt.% were discarded, since they hindered the dispersion of nanotubes within the polymer and adversely affected the viscosity of the sensing film. Moreover, a growing number of nanoparticles within the polymer layer increased the chances of short-circuiting between electrode plates, compromised the coating process, and contributed to a less stable

and repetitive response of the sensor over time. Therefore, in this work, a concentration of 1.0 wt.% of MWCNTs was considered optimum in terms of performance, signal stability, repeatability, and low baseline noise.

Upon absorption of VOCs, the conductive paths originally established by the MWCNTs are partially destroyed, which causes an increase in the resistivity of the sensing film. This process is reversible and nanoparticles tend to go back to their original position, once the desorption of analytes is completed. Hence, the performance of polymer composites is very dependent on the degree of analytes' absorption. Analytes with a higher absorption rate will contribute to greater disruption of the conductive network provided by nanotubes, which should result in a higher sensor response. With some of the tested compounds, a slight decay of the response signal was detected over time, which can be attributed to the fast absorption/ desorption of analytes from the polymer layer (see Supporting Information).

3.3. Selective Response of Hybrid and Pristine Polymer Films

The response of hybrid films containing 1.0 wt.% of MWCNTs was evaluated and compared to the performance of pristine PDMS sensors of 25 μm thickness. The raw values of sensitivities (S) and response times (δt) obtained for each of the sensors are gathered in **Table 2**, together with the corresponding LoD and the calculated relative selectivity (s). As expected, hybrid polymer films improved the sensitivity of the sensor significantly, compared to single PDMS materials. With the addition of only 1.0 wt.% of MWCNTs, the average sensitivity increased by a factor of 12, 10, or 2, in the detection of ethyl acetate, IPA and methanol respectively. In addition, hybrid nanocomposites also improved the average time response of the sensor, which was reduced approximately by half in the detection of all VOCs. The biggest sensitivity was recorded in the presence of toluene, which increased by a factor of 1000 compared to pristine PDMS materials. This dramatic rise in sensitivity can be explained due to the strong affinity between PDMS and toluene, as well as the special $\pi-\pi$

Table 2. Calculated sensitivity (S), LoD, response times (δt), and relative selectivity (s) of pristine 25 μm -PDMS sensors compared to hybrid 1.0 wt.% MWCNTs-PDMS sensors, in presence of tested VOCs and relative humidity (RH). Mean values at a frequency of 10 kHz.

Analyte	Concentration [ppm]	25 μm -PDMS sensors				[1.0 wt.%] MWCNTs-PDMS sensors			
		S [$\Omega \text{ ppm}^{-1}$]	LoD [ppm]	δt [min]	s	S [$\Omega \text{ ppm}^{-1}$]	LoD [ppm]	δt [min]	s
IPA	19000	-0.031	3319	49.17	1.00	0.325	314	20.83	1.00
EthAc	14900	-0.053	1938	12.96	1.71	0.675	152	5.83	2.07
MeOH	24000	-0.020	5136	58.10	0.65	0.056	1835	28.33	0.17
Toluene	17100	-0.002	–	45.01	0.05	1.872	55	16.67	5.75
DI water	≈ 20000 ^{a)}	-0.029	3517	74.81	0.94	0.051	1998	44.82	0.16

^{a)} Triggered a corresponding rise in RH levels of $\approx 20\%$.

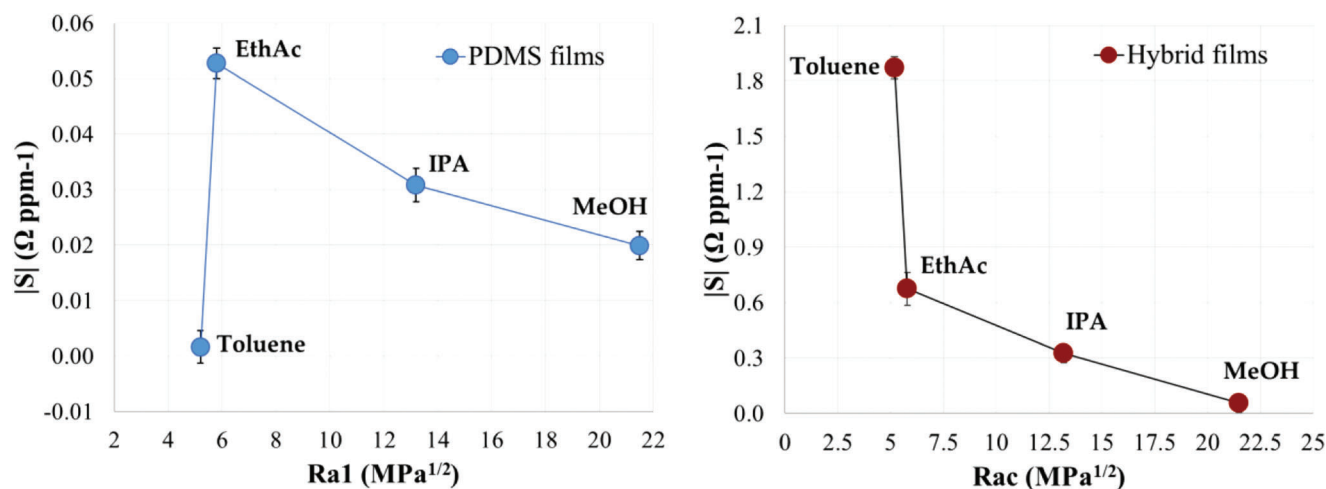


Figure 8. Sensitivity (S) of pristine (left) and hybrid (right) PDMS films versus the polymer-analyte affinity expressed by means of the R_a value.

interactions occurring at the surface of the carbon nanotubes with toluene's aromatic ring in its molecular structure.^[76] Measured improvements in sensitivity and response times triggered by the addition of nanoparticles were more noticeable towards analytes with a strong PDMS affinity, such as ethyl acetate or toluene than analytes with low affinity, such as methanol. Therefore, the addition of MWCNTs was proven to enhance the selectivity of PDMS films towards non-polar or weakly polar compounds. This behavior is also evident when analyzing and comparing the relative selectivity of the films.

The selectivity of pristine and hybrid polymer films has been analyzed by means of the Hansen solubility parameters and the R_a value. The single interaction between PDMS films and analytes is evaluated with the R_a values of the polymer (R_{a_1}), whereas the interaction of hybrid polymer composites with analytes is evaluated with the combined R_a values (R_{a_c}) obtained after the addition of MWCNTs. As it was stated before, due to the low concentration of MWCNTs added into the polymer layer, differences in solubility and, therefore, in the R_a values of single and hybrid polymer films are almost non-existent. In **Figure 8**, it can be clearly seen that the response of both, pristine and hybrid polymer composites was highly determined by the type of analytes to be detected. In general, analytes with solubility parameters similar to those of PDMS (low R_a) displayed a greater sensitivity than analytes with disparate parameters (high R_a). This behavior was

already depicted in the response of pristine PDMS films, with the exception of toluene, due to the high dependency of these sensors on the electrical permittivity of analytes. This limitation was clearly solved with the addition of conductive nanoparticles inside the polymer layer. Hybrid polymer films detach permittivity changes of the polymer from the detection principle of the device, so that polymer-analyte affinity can be better correlated with the chemoresistive response of the sensor. Thus, analytes with a stronger PDMS affinity caused a major disturbance to the conductive network provided by the nanotubes and, therefore, a higher sensitivity was recorded. MWCNTs also contributed to improving the selective response of PDMS films, because of the non-polar nature of carbon nanoparticles and the special interaction with some analytes occurring at the surface of nanotubes, which, for instance, explains the outstanding sensitivity of hybrid polymer films towards toluene.

The effect of polymer-analyte affinity was also measured to have an impact on the time response of the device. In general, analytes with a strong PDMS interaction (low R_a) displayed a faster absorption/desorption process from the polymer membrane compared to analytes with a soft interaction (high R_a) (see **Figure 9**). Hybrid polymer composites maintained a similar trend to organic compounds, but the times recorded were half as fast compared to pristine polymeric films. This reduction in the times could be attributed to an increase in the porosity of the polymer

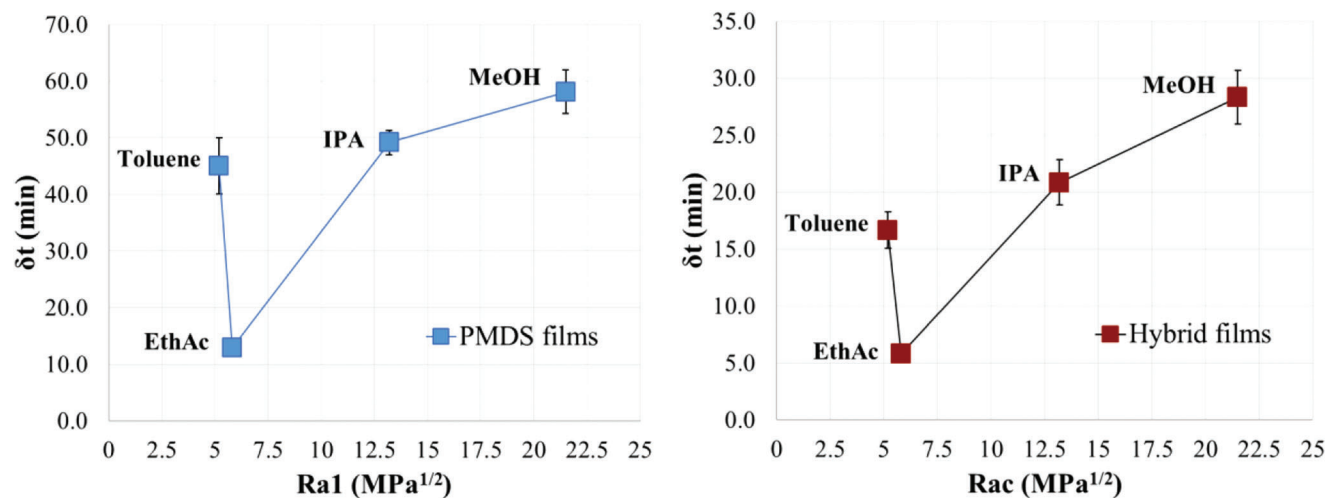


Figure 9. Time response (δt) of pristine (left) and hybrid (right) PDMS films versus the polymer-analyte affinity expressed by means of the R_a value.

caused by the addition of nanoparticles; or the fact that hybrid films are more sensitive and, therefore, they are able to detect faster small changes in the polymer membrane caused by the absorption of analytes.

Even though there is a clear correlation between polymer-analyte affinity (R_a value) and the performance of the sensor, this has been proven to be far from linear. Discrepancies in this relationship might be explained by the effect of nanofillers, for instance. The special interaction between MWCNTs and toluene was already reported as the main cause for the outstanding sensitivity of hybrid films towards this analyte. Other factors that can explain deviations in this relationship might be more related to the different chemical properties of analytes, such as their vapor pressure or molecular size. Theoretically, high pressures promote better and faster absorption of analytes into the polymer layer. In addition, large molecules tend to be less effective than smaller species in their dissolution with polymers. All these factors might explain why the time response of the sensor towards toluene is very similar to toward IPA, the excellent response of the sensor towards ethyl acetate, or why differences in sensitivity between IPA and methanol are not better featured, despite of their clear differences in the solubility parameters.

Last but not least, since all fabricated sensors have the ability to operate at room temperature, the effect of relative humidity (RH) was also analyzed. Despite of the hydrophobic nature of PDMS; RH was measured to have an impact on the response of both, pristine and hybrid polymer films. Therefore, RH and ambient temperature were carefully controlled in all the experiments conducted. The influence of RH was more notorious in pristine PDMS films, especially at low polymer thicknesses, due to the adsorption of high-permittivity water vapor molecules. The impact of RH was minimized with the addition of MWCNTs into the polymer layer. Deviations caused by RH were small in the response of hybrid films compared to pristine PDMS sensors. Again, this effect could be associated with the hydrophobicity provided by PDMS, and the fact that hybrid films detach permittivity changes from the detection principle of the device (see section 6 of the supporting material).

4. Conclusion

This work has successfully implemented a methodology based on the HSPs, to analyze the selectivity of both, pristine and hybrid polymeric materials in presence of common vapor analytes. Even though the calculation of HSPs depends on a great extent to the data available for polymers, nanofillers, and vapor analytes, the method proposed in this work outlines great potential in the selection of suitable polymeric materials for the discrimination of VOCs.

In the analysis of hybrid polymer composites, PDMS films containing 1.0 wt.% of MWCNTs displayed the most optimum and stable performance over time. With such a small concentration of nanofillers, the selectivity of the composite is still governed by the polymer, yet it is possible to achieve a significant improvement in the overall performance of the sensor. Therefore, this work has proven that with the proper selection of the polymer, and the addition of carbon nanoparticles at low concentrations, it is possible to obtain a highly sensitive membrane with the desired selectivity for a specific application. It is worth mentioning that solubility parameters alone sometimes fell short to explain the whole interaction between polymer composites and VOCs. Other factors should also be considered, such as the vapor pressure of analytes, the detection principle of the device, or special intermolecular interactions occurring between analytes and the nanoparticles. In this work, the best responses were obtained in presence of toluene, due to its strong affinity with PDMS, but also the special π - π interactions occurring at the surface of multiwalled carbon nanotubes.

Supporting Information

Supporting Information is available from the Wiley Online Library or from the author.

Acknowledgements

The authors of this work are thankful to SEAT S.A. for their support during the whole research project without further incidences or conflicts of

interest. This work was supported by the Catalan Ministry of Business and Labour (2018 DI 0102) and the EIT Urban Mobility, European Commission (I-2020-31 20007).

Conflict of Interest

The authors declare no conflict of interest.

Data Availability Statement

The data that support the findings of this study are available from the corresponding author upon reasonable request.

Keywords

gas sensors, hybrid polymers, selectivity, solubility parameters, volatile organic compounds (VOCs)

Received: August 3, 2022

Revised: October 3, 2022

Published online:

- [1] J. Pereira, P. Porto-Figueira, C. Cavaco, K. Taunk, S. Rapole, R. Dhakne, H. Nagarajaram, J. S. Câmara, *Metabolites* **2015**, *5*, 3.
- [2] A. T. Güntner, S. Abegg, K. Königstein, P. A. Gerber, A. Schmidt-Trucksäss, S. E. Pratsinis, *ACS Sens.* **2019**, *4*, 268.
- [3] J. Faber, K. Brodzik, *AIMS Environ. Sci.* **2017**, *4*, 112.
- [4] S. K. Jha, K. Hayashi, *Int. J. Mass Spectrom.* **2017**, *415*, 92.
- [5] H. Nazemi, A. Joseph, J. Park, A. Emadi, *Sensors* **2019**, *19*, 1285.
- [6] N. Joshi, T. Hayasaka, Y. Liu, H. Liu, O. N. Oliveira, L. Lin, *Microchim. Acta* **2018**, *185*, <https://doi.org/10.1007/s00604-018-2750-5>.
- [7] E. P. Ollé, J. Farré-Lladós, J. Casals-Terré, *Sensors* **2020**, *20*, 5478.
- [8] F. Meng, X. Shi, Z. Yuan, H. Ji, W. Qin, Y. B. Shen, C. Xing, *Sens. Actuators, B* **2022**, *350*, 130867.
- [9] H. Fan, X. Jia, *Solid State Ionics* **2011**, *192*, 688.
- [10] Z. Wu, H. Zhang, H. Ji, Z. Yuan, F. Meng, *J. Alloys Compd.* **2022**, *918*, 165510.
- [11] Y. Xing, L.-X. Zhang, M.-X. Chong, Y.-Y. Yin, C.-T. Li, L.-J. Bie, *SSRN Electron. J.* **2022**, *369*, 132356.
- [12] S. Some, Y. Xu, Y. Kim, Y. Yoon, H. Qin, A. Kulkarni, T. Kim, H. Lee, *Sci. Rep.* **2013**, *3*, 1868.
- [13] B. Yoon, S. -J. Choi, T. M. Swager, G. F. Walsh, *ACS Sens.* **2021**, *6*, 3056.
- [14] M. N. Norizan, M. H. Moklis, S. Z. Ngah Demon, N. A. Halim, A. Samsuri, I. S. Mohamad, V. F. Knight, N. Abdullah, *RSC Adv.* **2020**, *10*, 43704.
- [15] S. Cichosz, A. Masek, M. Zaborski, *Polym. Test.* **2018**, *67*, 342.
- [16] Y. Yan, G. Yang, J. -L. Xu, M. Zhang, C. -C. Kuo, S. -D. Wang, *Sci. Technol. Adv. Mater.* **2020**, *21*, 768.
- [17] M. Hussain, S. Hasnain, N. A. Khan, S. Bano, F. Zuhra, M. Ali, M. Khan, N. Abbas, A. Ali, *Polymers* **2021**, *13*, 3019.
- [18] R. Blue, Z. Vobecka, P. J. Skabara, D. Uttamchandani, *Sens. Actuators, B* **2013**, *176*, 534.
- [19] S. Ramanathan, M. Jusoh, T. Sabapathy, M. N. Yasin, S. C. B. Gopinath, H. Arahim, M. N. Osman, Y. A. Wahab, *Appl. Phys. A: Mater. Sci. Process.* **2020**, *126*, 1.
- [20] Q. N. Minh, H. D. Tong, A. Kuijk, F. Van De Bent, P. Beekman, C. J. M. Van Rijn, *RSC Adv.* **2017**, *7*, 50279.
- [21] M. Kitsara, D. Goustouridis, S. Chatzandroulis, M. Chatzichristidi, I. Raptis, T. Ganetsos, R. Igreja, C. J. Dias, *Sens. Actuators, B* **2007**, *127*, 186.
- [22] P. Oikonomou, I. Raptis, M. Sanopoulou, *Sensors* **2014**, *14*, 16258.
- [23] Y. Jiang, N. Tang, C. Zhou, Z. Han, H. Qu, X. Duan, *Nanoscale* **2018**, *10*, 20578.
- [24] S. Badhulika, N. V. Myung, A. Mulchandani, *Talanta* **2014**, *123*, 109.
- [25] A. Jahangiri-Manesh, M. Mousazadeh, M. Nikkhal, S. Abbasian, A. Moshaii, M. J. Masroor, P. Norouzi, *Microchem. J.* **2022**, *173*, 106988.
- [26] I. Constantinoiu, C. Viespe, *Coatings* **2019**, *9*, 373.
- [27] Q. Nguyen Minh, A. Kuijk, S. P. Pujari, F. van de Bent, J. Baggerman, H. D. Tong, H. Zuilhof, C. J. M. van Rijn, *Sens. Actuators, B* **2017**, *252*, 1098.
- [28] S. Dissanayake, C. Vanlangenberg, S. V. Patel, T. Mlsna, *Sens. Actuators, B* **2015**, *206*, 548.
- [29] J. M. Kalaw, F. B. Sevilla Iii, *Holzforchung* **2018**, *72*, 215.
- [30] Y. Zheng, H. Li, W. Shen, J. Jian, *Sens. Actuators, A* **2019**, *285*, 395.
- [31] P. Oikonomou, A. Botsialas, N. Papanikolaou, I. Kazas, K. Ntetsikas, G. Polymeropoulos, N. Hadjichristidis, M. Sanopoulou, I. Raptis, *IEEE Sens. J.* **2020**, *20*, 463.
- [32] Z. Wang, A. Syed, S. Bhattacharya, X. Chen, U. Buttner, G. Iordache, K. Salama, T. Ganetsos, E. Valamontes, A. Georgas, I. Raptis, P. Oikonomou, A. Botsialas, M. Sanopoulou, *Microelectron. Eng.* **2020**, *225*, 111253.
- [33] M. Paknahad, C. McIntosh, M. Hoorfar, *Sci. Rep.* **2019**, *9*, 161.
- [34] J. N. Lee, C. Park, G. M. Whitesides, *Anal. Chem.* **2003**, *75*, 6544.
- [35] E. D. Skutin, S. O. Podgorniy, O. T. Podgornaya, N. S. Kolyanichev, A. A. Katkov, *J. Phys.: Conf. Ser.* **2018**, *944*, 012110.
- [36] S. Jenkins, *Hansen solubility parameters: a user's handbook*, (Ed: C. M. Hansen), **2011**, pp 1–24.
- [37] P. Slobodian, P. Riha, A. Lengalova, P. Svoboda, P. Saha, *Carbon* **2011**, *49*, 2499.
- [38] M. Babaei, N. Alizadeh, *Sens. Actuators, B* **2013**, *183*, 617.
- [39] C. V. Rumens, M. A. Ziai, K. E. Belsey, J. C. Batchelor, S. J. Holder, *J. Mater. Chem. C* **2015**, *3*, 10091.
- [40] S. Detriche, G. Zorzini, J.-F. Colomer, A. Fonseca, J. B. Nagy, *J. Nanosci. Nanotechnol.* **2008**, *8*, 6082.
- [41] J. Ma, X. Nan, J. Liu, W. Zhu, W. Qin, *Mater. Today Commun.* **2018**, *14*, 99.
- [42] S. Pu, Y.-B. Hao, X.-X. Dai, P.-P. Zhang, J.-B. Zeng, M. Wang, *Polym. Test.* **2017**, *63*, 289.
- [43] J. Ma, R. M. Larsen, *J. Thermoplast. Compos. Mater.* **2012**, *27*, 801.
- [44] J. R. Tao, D. Yang, Y. Yang, Q.-M. He, B. Fei, M. Wang, *Polymer* **2022**, *252*, 124963.
- [45] J. H. Kim, J. Y. Hwang, H. R. Hwang, H. S. Kim, J. H. Lee, J. W. Seo, U. S. Shin, S. H. Lee, *Sci. Rep.* **2018**, *8*, 1375.
- [46] V. Balasubramani, S. Sureshkumar, T. S. Rao, T. M. Sridhar, *ACS Omega* **2019**, *4*, 9976.
- [47] A. Olean-Oliveira, M. F. S. Teixeira, *Sens. Actuators, B* **2018**, *271*, 353.
- [48] V. Balasubramani, S. Chandraleka, T. S. Rao, R. Sasikumar, M. R. Kuppusamy, T. M. Sridhar, *J. Electrochem. Soc.* **2020**, *167*, 037572.
- [49] F. Schipani, D. R. Miller, M. A. Ponce, C. M. Aldao, S. A. Akbar, P. A. Morris, *Adv. Sci.* **2016**, *5*, 86.
- [50] N. Sankar, M. N. Reddy, R. K. Prasad, *Bull. Mater. Sci.* **2016**, *39*, 47.
- [51] V. Schroeder, S. Savagatrup, M. He, S. Lin, T. M. Swager, *Chem. Rev.* **2019**, *119*, 599.
- [52] K. Berean, J. Z. Ou, M. Nour, K. Latham, C. Mcsweeney, D. Paull, A. Halim, S. Kentish, C. M. Doherty, A. J. Hill, K. Kalantar-Zadeh, *Sep. Purif. Technol.* **2014**, *122*, 96.
- [53] S. Khan, S. Ali, A. Bermak, *IEEE Access* **2019**, *7*, 134047.
- [54] M. Itagaki, S. Suzuki, I. Shitanda, K. Watanabe, *Electrochemistry* **2007**, *75*, 649.
- [55] J. Stagnus, I. M. Aerts, Z.-Y. Chang, G. C. M. Meijer, L. C. P. M. De Smet, E. J. R. Sudhölter, *Sens. Actuators, B* **2013**, *184*, 130.
- [56] D. Locatelli, V. Barbera, L. Brambilla, C. Castiglioni, A. Sironi, M. Galimberti, *Nanomaterials* **2020**, *10*, 1176.
- [57] S. D. Bergin, Z. Sun, D. Rickard, P. V. Streich, J. P. Hamilton, J. N. Coleman, *ACS Nano* **2009**, *3*, 2340.

- [58] J. C. Zuaznabar-Gardona, A. Fragoso, *J. Mol. Liq.* **2019**, 294, 111646.
- [59] J. Ma, L. Zhou, *Polym. Bull.* **2012**, 68, 1053.
- [60] S. Detriche, J. B. Nagy, Z. Mekhalif, J. Delhalle, *J. Nanosci. Nanotechnol.* **2009**, 9, 6015.
- [61] J. E. Mark, in *Polymer Data Handbook*, Oxford University Press, **1999**, pp. 411–431.
- [62] S. Ata, T. Yamada, K. Hata, *J. Nanosci. Nanotechnol.* **2017**, 17, 3310.
- [63] A. Nika, P. Oikonomou, T. Manouras, P. Argitis, M. Vamvakaki, M. Sanopoulou, I. Raptis, M. Chatzichristidi, *Microelectron. Eng.* **2020**, 227, 111304.
- [64] F. J. Romero, A. Rivadeneyra, A. Salinas-Castillo, A. Ohata, D. P. Morales, M. Becherer, N. Rodriguez, *Sens. Actuators, B* **2019**, 287, 459.
- [65] M. K. Filippidou, M. Chatzichristidi, S. Chatzandroulis, *Sens. Actuators, B* **2019**, 284, 7.
- [66] *Int. Conf. on Smart Instrumentation, Measurement and Applications*, (Eds: H. Omran, K. N. Salama), IEEE, New York, **2015**.
- [67] R. Igreja, C. J. Dias, *Mater. Sci. Forum* 455-456 **2004**, 455-456, 420.
- [68] R. Igreja, C. J. Dias, *Sens. Actuators, A* **2011**, 172, 392.
- [69] R. Igreja, C. J. Dias, *Sens. Actuators, B* **2006**, 115, 69.
- [70] R. Igreja, C. J. Dias, *Sens. Actuators, A* **2004**, 112, 291.
- [71] J. T. W. Yeow, Y. Wang, *J. Sens.* **2009**, 2009., 493904.
- [72] I. V. Zaporotskova, N. P. Boroznina, Y. N. Parkhomenko, L. V. Kozhitov, *Mod. Electron. Mater.* **2016**, 2, 95.
- [73] S. Kumar, V. Pavelyev, P. Mishra, N. Tripathi, *Sens. Actuators, A* **2018**, 283, 174.
- [74] L. Vigna, A. Fasoli, M. Cocuzza, F. C. Pirri, L. D. Bozano, M. Sangermano, *Macromol. Mater. Eng.* **2019**, 304, 1800453.
- [75] D. Wu, M. Wei, R. Li, T. Xiao, S. Gong, Z. Xiao, Z. Zhu, Z. Li, *Composites, Part B* **2019**, 174, 107034.
- [76] E. M. Pérez, N. Martín, *Chem. Soc. Rev.* **2015**, 44, 6425.